Global and Planetary Change 234 (2024) 104367

Contents lists available at ScienceDirect

Global and Planetary Change

journal homepage: www.elsevier.com/locate/gloplacha

Interannual variations in stable isotopes of atmospheric water in arid Central Asia due to changes in atmospheric circulation

Shengjie Wang [a,b], Gahong Yang [a], John Bershaw [c], Xiaokang Liu [d], Kei Yoshimura [e], Yanqiong Xiao [a], Mingjun Zhang [a,*]

[a] Key Laboratory of Resource Environment and Sustainable Development of Oasis of Gansu Province, College of Geography and Environmental Science, Northwest Normal University, Lanzhou 730070, China
[b] Laboratoire de Météorologie Dynamique, IPSL, CNRS, Sorbonne Université, Paris 75006, France
[c] Portland State University, Portland, OR 97201, USA
[d] School of Geographic and Environmental Sciences, Tianjin Normal University, Tianjin 300387, China
[e] Atmosphere and Ocean Research Institute, University of Tokyo, Tokyo 169-8555, Japan

ARTICLE INFO

Handling Editor: Trude Storelvmo

Keywords:
Stable isotope
Central Asia
Mid-latitude Westerlies
Atmospheric circulation
Temperature effect

ABSTRACT

The oxygen isotope compositions in atmospheric water including water vapor and precipitation have been widely used to trace moisture sources and to reconstruct past climates. However, the environmental controls of stable isotopes in atmospheric water depend on the time scales. Because of limited observations in arid Central Asia, factors controlling interannual variations in atmospheric water isotopes are still not clear. Using an isotope-enabled general climate model, we do not find at the annual scale the significant relationship between temperature and $\delta^{18}O$ values during 1979–2020 that is usually observed at the monthly scale. Under a warming background, there is no significant enriching trend in water isotopes. We found a strong positive correlation between westerly (and southerly) water vapor flux and $\delta^{18}O$ values on an interannual scale for the area between 35°N–50°N and 50°E–80°E in the upstream direction. High and low $\delta^{18}O$ years are characterized by different atmospheric circulations of mid-latitude Westerlies, and do not always correspond to the warm and cold years respectively. When the prevailing Westerlies are enhanced, the Westerlies circulation may carry more water vapor from the lower latitudes, leading to higher $\delta^{18}O$ values in Central Asia. The changes in Westerlies circulation are supported by the clustered backward trajectories during enriched and depleted years. The limited precipitation isotope observations also show similar findings as the simulations on an interannual scale. The interannual variations of stable isotopes in atmospheric water in arid Central Asia reflect the changes in the mid-latitude Westerlies circulation. This should be taken into account when interpreting oxygen isotope proxies of paleoclimate records.

1. Introduction

Atmospheric water including water vapor and precipitation is an important part of the water cycle with a significant impact on water resources (Konapala et al., 2020; Thackeray et al., 2022). As an integrated natural tracer, the oxygen isotopic compositions ($\delta^{18}O$) of atmospheric water are useful for assessing source-sink dynamics of global water (Bowen et al., 2019). The stable isotopes in water vapor and precipitation have been used to understand atmospheric circulation (Araguás-Araguás et al., 1998; Chiang et al., 2020; Man et al., 2022), identify moisture sources (Wang et al., 2017; Gimeno et al., 2020; Welp et al., 2022), and distinguish contributions from advected versus locally recycled moisture to precipitation (Dar et al., 2021; Zhang et al., 2021; Gui et al., 2022). In paleoclimate studies, stable oxygen isotopes in ice cores, tree rings, speleothems and other ancient water proxies are used to examine historical air temperature, precipitation, monsoon activities, and droughts (Thompson et al., 1997, 2018; Cheng et al., 2016a; Xu et al., 2021; Parker et al., 2021). These require a thorough understanding of modern water isotopes in atmospheric water which are connected to climate proxies (Baker et al., 2019; Markle and Steig, 2022).

Central Asia is located far from oceans and is characterized by an arid

* Corresponding author.
E-mail address: mjzhang2004@163.com (M. Zhang).

https://doi.org/10.1016/j.gloplacha.2024.104367
Received 11 June 2023; Received in revised form 30 December 2023; Accepted 20 January 2024
Available online 1 February 2024

climate with fragile ecosystems mainly comprising of oases, deserts, and steppes. Water is an important but limited resource for the region, constraining human living environments (Chen et al., 2022a; Huang et al., 2022). Most inhabitants live in oases surrounded by desert, and a deficit between water supply and demand is prominent (Chen et al., 2022c; Xue et al., 2022). Changes in precipitation and sources of water vapor feeding Central Asia have been topics in a changing climate (Shen et al., 2022; Yao et al., 2022). The water vapors transported by mid-latitude Westerlies and monsoons drive hydrological changes in this region on various time scales (Rao et al., 2019; Chen et al., 2021), providing a stable isotope perspective on this topic (Zhang, 2021). In arid Central Asia, stable oxygen isotopes in modern precipitation and water vapor are enriched in summer and depleted in winter, which is mainly controlled by temperature (also known as the temperature effect) rather than precipitation amount on an intra-annual timescale (Liu et al., 2014; Wang et al., 2016, 2019, 2022). This temperature effect on stable isotopes in precipitation is used to interpret oxygen isotope compositions in paleoclimate proxies, such as Central Asian ice cores (Thompson et al., 1997; Tian et al., 2006). For example, annual $\delta^{18}O$ values in an ice core from the eastern Pamir positively correlate with air temperature, indicating that isotopic compositions are an important indicator of local temperature (Tian et al., 2006).

However, interpretations of oxygen isotopes in paleoclimate proxies are not always consistent, including ice cores and speleothems. Paleoclimate records generally show relatively lower $\delta^{18}O$ values during the interglacials (or warm period) and higher $\delta^{18}O$ values during the glacials (or cold period), which contrasts with the abovementioned positive correlation between $\delta^{18}O$ values and temperature. Liu et al. (2015) showed that variations of $\delta^{18}O$ values in precipitation and ice cores are negatively correlated with changes in temperature on interannual to decadal timescale in Central Asia. Moreover, recent studies suggested that atmospheric circulation signals, rather than temperature or precipitation amount, have dominated changes in modern precipitation isotopes on annual or longer timescales, with different paths of water vapors may be associated with distinct isotopic compositions (Shi et al., 2021; Zhang, 2021). This is supported by many climate studies which revealed a connection between precipitation and large-scale moisture transport in arid Central Asia (Peng et al., 2020; Shen et al., 2022; Guan et al., 2022). Such observations between variations in atmospheric circulation and $\delta^{18}O$ values have been referred to interpret paleo-isotope records such as the Asian speleothems (Cheng et al., 2016b; Cai et al., 2017) and tree rings (Xu et al., 2014, 2018). To accurately interpret the climatic significance of $\delta^{18}O$ on both intra- and interannual scales, isotope-enabled numerical simulations with good spatial coverage and extended time have shown utility (Gao et al., 2016; Yu et al., 2021; Bühler et al., 2022).

To better understand the controlling factors of stable oxygen isotopes in atmospheric water on interannual time scales in arid Central Asia, we examine intra- and interannual simulations in arid Central Asia using an isotope-enabled general circulation model. We also investigate the relationship between water vapor fluxes and precipitable water $\delta^{18}O$ values on an interannual scale, and discuss the air regimes associated with enriched or depleted isotopes. Our findings are useful for understanding the relationship between westerly moisture transport and stable water isotope values, and provide a linkage of isotopic controls on different time scales.

2. Data and methods

2.1. Study area

Arid Central Asia (Fig. 1) is dominated by mid-latitude Westerlies all year round. The water vapor flux is small in winter, and surface air is relatively dry and cold; in contrast, water vapor transport in summer is much higher than in winter. Consistent with the seasonality of water vapor flux, most of the precipitation occurs from April to October (Bershaw, 2018; Yao et al., 2022). In this azonal arid region, the Tianshan Mountains act as a typical water tower with annual precipitation higher than 400 mm which is much larger than the nearby Taklimakan and Gurbantunggut deserts. The rivers and streams from the high altitudes constitute the vital water resources that are essential for the regional sustainability of oases. In addition, various paleoclimate archives such as speleothems, tree rings, loess sections and ice cores have been derived in the Tianshan Mountains (Chen et al., 2019), which are helpful to understand the evolutions of environment and climate in Central Asia on long-term timescales.

2.2. Simulated $\delta^{18}O$ database

The isotope-incorporated Global Spectral Model version 2 (isoGSM2)

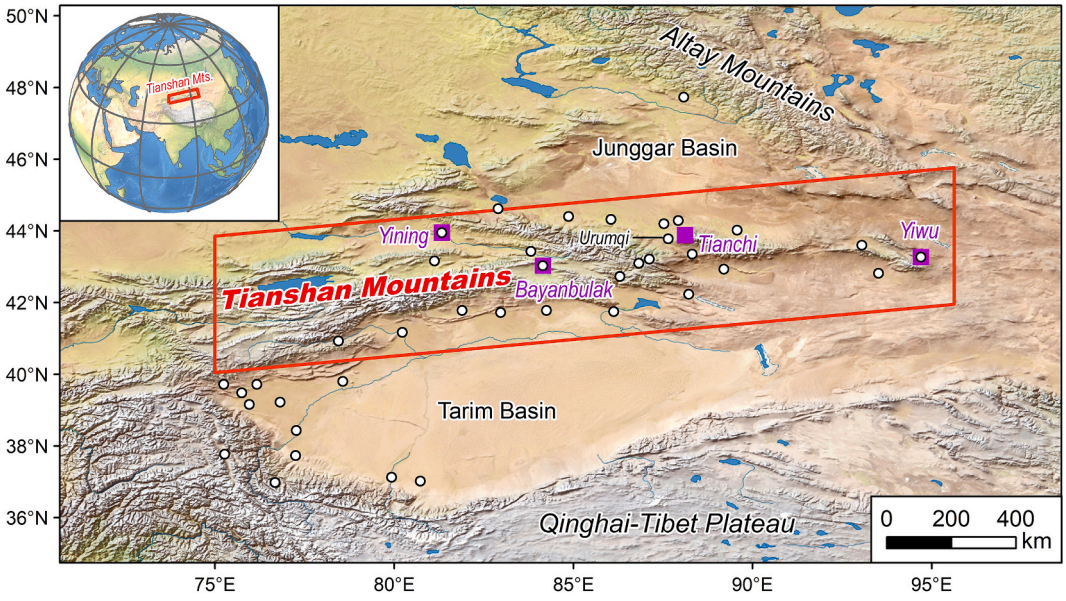

Fig. 1. Location of precipitation isotope sampling stations (white circles) and temperature observation stations (purple squares) across the Tianshan Mountains of arid Central Asia. The red frame denotes the Tianshan Mountains. (For interpretation of the references to colour in this figure legend, the reader is referred to the web version of this article.)

(Yoshimura et al., 2008) was used to examine stable isotope variability across the Tianshan Mountains from 1979 to 2020. The spatial resolution is 1.905° (latitude) × 1.875° (longitude). This model has been widely used to investigate atmospheric processes (Chiang et al., 2020; Kathayat et al., 2022; Zhang et al., 2023; Liu et al., 2023).

The oxygen isotope ratios are expressed in delta notation relative to the Vienna Standard Mean Ocean Water:

$$\delta = \left(R_{\text{sample}}/R_{\text{V-SMOW}}-1\right) \times 1000‰, \quad (1)$$

where R_{sample} represents the isotope ratio of $^{18}O/^{16}O$ in samples, and $R_{\text{V-SMOW}}$ represents the isotope ratio of $^{18}O/^{16}O$ in Vienna Standard Mean Ocean Water. The monthly $\delta^{18}O$ data were averaged to an annual basis weighted by the precipitation amount. Considering the significant positive correlation between isotopes in precipitation and precipitable water (Fig. S1), and the temporal continuity of water vapor isotopes in an arid climate (Fig. S2), here we mainly used the simulations of precipitable water isotopes. Similar procedures using weighted water vapor isotopes instead of weighted precipitation isotopes were conducted in previous works (e.g., Zhang et al., 2023).

2.3. Observed $\delta^{18}O$ database

To evaluate the monthly series of simulated isotopes, we collected precipitation $\delta^{18}O$ data (Fig. 1 and Table S1) on a monthly scale at 39 stations (Tian et al., 2007; Pang et al., 2011; Yao et al., 2013; Liu et al., 2014; Wang et al., 2016, 2019, 2022; Sun et al., 2016, 2019; Shi et al., 2021; Song et al., 2022; IAEA, 2022). The isoGSM2-modeled isotopic compositions were weighted using precipitation amount when needed, and interpolated using a bilinear method to each observed location. The observed isotope compositions at different scales were also compiled into a weighted monthly series. When the precipitation amount was not provided in original data sources, we used the gridded daily precipitation product from the NOAA Climate Prediction Center (CPC) Global Unified Gauge-based Analysis of Daily Precipitation (Chen et al., 2008), a method employed by Putman et al. (2019). In addition, to assess the interannual performance of simulated isotopes, we used the multi-year observations in the GNIP (Global Network of Isotopes in Precipitation) Urumqi station (43.78°N, 87.62°E, 918 m) during 1986–2003. This is the only existing sampling station longer than 10 years in arid Central Asia.

2.4. Meteorological data

Here we used the ERA5 (the fifth-generation reanalysis data of the European Centre for Medium-Range Weather Forecasts; Hersbach et al., 2020) monthly specific humidity, zonal and meridional wind component and surface air pressure during the years 1979–2020, with a spatial resolution of 0.25° × 0.25°. To calculate water vapor flux, the vertical integration was conducted from the surface to 300 hPa. The water vapor flux represents the amount of water vapor flowing through the unit area per unit time, and is determined using the zonal and meridional water vapor flux.

To verify the temperature effect of stable water isotopes on intra- and interannual scales, we selected air temperature and precipitation amount data from four meteorological stations during 1979–2020 (Fig. 1), i.e., Yining (43.95°N, 81.33°E, 663 m), Bayanbulak (43.03°N, 84.15°E, 2458 m), Tianchi (43.88°N, 88.12°E, 1930 m) and Yiwu (43.27°N, 94.70°E, 1729 m).

The HYSPLIT (Hybrid Single-Particle Lagrangian Integrated Trajectory) model version 4 (Stein et al., 2015) and the NCEP/NCAR (National Centers for Environmental Prediction and National Center for Atmospheric Research) global reanalysis data with a spatial resolution of 2.5° × 2.5° (Kalnay et al., 1996) were used to trace the backward trajectories to Central Asia during the enriched or depleted years of stable water isotopes. The starting heights were set as 500 m and 1500 m above ground level, and the back duration of these daily trajectories from 00 UTC is set as 5 days (120h) which is generally consistent with a specific humidity-adjusted method in Central Asia (Wang et al., 2017). The optimal cluster number in cluster analysis is based on the total spatial variance in the model.

3. Results and discussion

3.1. Assessment of simulations

We assessed the performance of isoGSM2 across the Tianshan Mountains at both the monthly and annual scales. At the monthly scale, we tested the performance against compiled $\delta^{18}O$ data at 39 stations. Comparing the measured monthly averages of precipitation isotopes and isoGSM2-derived precipitable water isotopes (Fig. 2), there is a positive correlation between the measurements and simulations ($r = 0.66$), which is statistically significant at the 0.01 level, showing the variability of measured and simulated $\delta^{18}O$ was generally consistent.

At the annual scale, we used the multi-year observations in the GNIP Urumqi station during 1986–2003 (IAEA, 2022; Fig. 3). There is a significant positive correlation between the measured precipitation isotopes and isoGSM-simulated precipitable water isotopes ($r = 0.88$, $p < 0.01$, $n = 12$). The model is able to capture the large-scale drivers controlling the isotopic composition of water vapor as shown in Fig. 3. The validations at the sampling stations (Figs. 2 and 3) as well as the linear relationship between precipitation isotopes and water vapor isotopes (Fig. S1) therefore suggest isoGSM2 can be applied to describe the annual and seasonal variation of $\delta^{18}O$ in precipitation of arid Central Asia.

3.2. Inconsistent temperature effect: intra- and interannual basis

For the four stations in arid Central Asia, there are clear seasonal variations in isotopes, where stable oxygen isotopes are relatively enriched in summer with a higher temperature and depleted in winter with a lower temperature (Fig. S3). In these stations, the maximum $\delta^{18}O$ occurs from June to July, and the minimum appears in January. Most stations have an annual offset >10‰. Under a typical temperate continental climate, the maximum temperature is always seen in July and the minimum occurs in January. Among the four stations, Bayanbulak is the coldest station due to the high altitudes. There is a strong positive correlation between monthly $\delta^{18}O$ and air temperature, also known as the

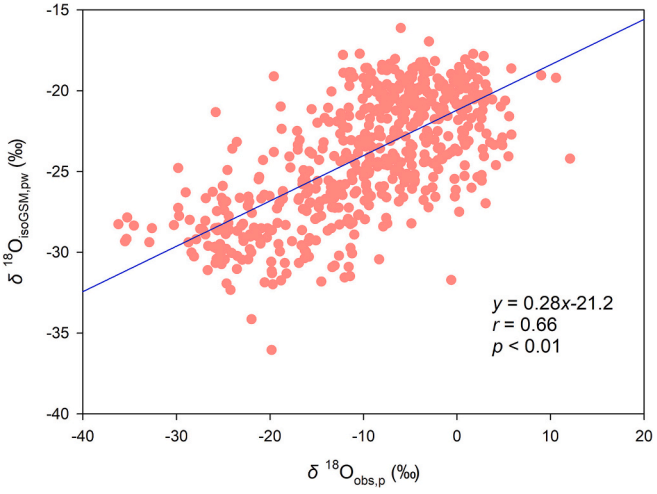

Fig. 2. Relationship between observed precipitation $\delta^{18}O$ (horizontal axis) and isoGSM2-simulated precipitable water $\delta^{18}O$ (vertical axis) at 39 precipitation isotope sampling stations across the Tianshan Mountains of arid Central Asia on a monthly scale. The linear regression line is also provided.

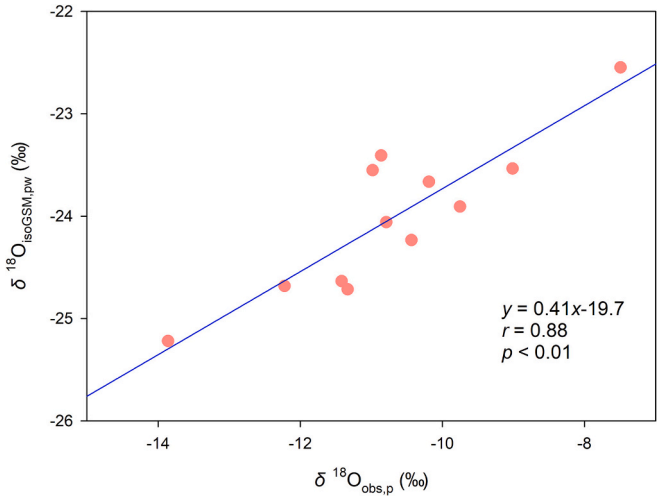

Fig. 3. Correlations between observed annual precipitation $\delta^{18}O$ in Urumqi and isoGSM2-simulated annual precipitable water $\delta^{18}O$ in the nearest grid box. The annual isotope values are weighted using observed precipitation amounts in Urumqi. The linear regression line is also provided.

temperature effect (Fig. 4a–d). All the linear regressions are statistically significant at the 0.01 level. This temperature effect is consistent with previous observations in arid Central Asia (Liu et al., 2014; Wang et al., 2016; Sun et al., 2019).

On an annual basis, the weighted annual $\delta^{18}O$ and air temperature show a weak relationship (Fig. 4e–h), which is starkly different from monthly results. In Tianchi and Yiwu, there are nonsignificant negative correlations that are opposite to the temperature effect. Table 1 and Fig. S4 show the relationship between isotope and temperature for each season. There is also no statistically significant correlation at the 0.05 level for each season. In summer with relatively more precipitation amounts (Fig. S4e-h), the correlation coefficients between isotope value and temperature on an inter-annual basis range between −0.04 (Yiwu) to 0.18 (Yining), which is much less than those on a monthly basis (0.94 to 0.97; Fig. 4a-d). Among the four stations, the Yining station with relatively weak seasonality of precipitation amount has a slightly larger correlation coefficient than the rest three stations on an annual basis, but the seasonal correlations are still weaker than the annual correlations (Table 1).

We provided the observed results in the GNIP Urumqi station in Table 1. On an annual scale, there is no significant correlation for these observed data ($r = -0.06$, $p = 0.84$, Fig. S5). The correlation coefficients are 0.11 in spring, −0.05 in summer, −0.35 in autumn and 0.29 in winter, which are also statistically nonsignificant. The simulated differences in the temperature effect at various temporal scales (Fig. 4) are supported by the observations in the GNIP Urumqi station.

Under a warming climate in the past decades (Yao et al., 2022), the traditional temperature effect predicts that the heavy isotopes might show an enriching trend as the temperature increases. As seen in our simulations (Fig. 5), $\delta^{18}O$ in four stations shows a linear trend ranging within ±0.1‰/decade, but the trends are not statistically significant. Research on ice cores in the eastern section of the Tianshan Mountains (Yang et al., 2018) also shows a depleting trend of −0.1‰/decade during 1979–2007, which is generally consistent with our results.

The isotopes in atmospheric water are associated with the local meteorological conditions or the remote factors along transport paths from moisture sources. In an arid setting, the below-cloud evaporation is usually highlighted and may enrich the heavy isotopes in raindrops in a warming background (Pang et al., 2011; Crawford et al., 2017; Graf et al., 2019). However, Wang et al. (2021) indicated that most areas across the Tianshan Mountains had a non-significant enhancing trend in below-cloud evaporation since 1960, which may raise the $\delta^{18}O$ values in precipitation. A regional factor, moisture recycling, usually modifies the $\delta^{18}O$ values in atmospheric water (Salati et al., 1979; Risi et al., 2013; Shi et al., 2022). In past decades, the actual precipitation amount contributed from the recycled moisture is still limited in many regional climate assessments (Wu et al., 2019; Yao et al., 2020), and the enhanced moisture advection plays a dominant role in the long term (Yao et al., 2022). Considering the estimated isotope compositions in advected and recycled vapor in Central Asia (Kong et al., 2013; Wang et al., 2022), the relatively low recycling ratio cannot greatly change the $\delta^{18}O$ values in past decades, and the potential regime of Westerlies

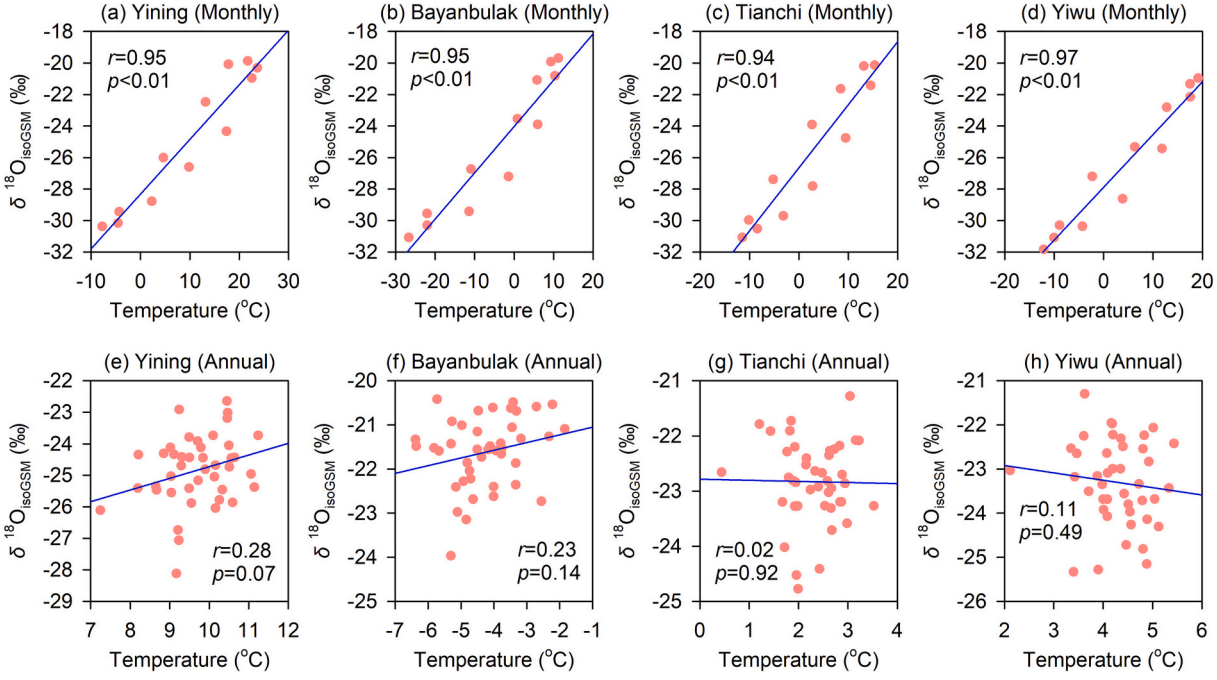

Fig. 4. Correlations between isoGSM2-simulated multi-annual-mean monthly (a–d) or annual (e–h) precipitation-weighted precipitable water $\delta^{18}O$ and observed air temperature at typical stations from 1979 to 2020. The linear regression lines for each station are also provided.

Table 1
Correlation coefficients between observed air temperature (T_{obs}) and isoGSM-simulated precipitation-weighted precipitable water $\delta^{18}O$ ($\delta^{18}O_{isoGSM,pw}$) or observed precipitation $\delta^{18}O$ ($\delta^{18}O_{obs,p}$) at typical stations for each season on an annual basis.

Data type	Station	Spring		Summer		Autumn		Winter		Annual	
		r	*p*	*r*	*p*	*r*	*p*	*r*	*p*	*r*	*p*
$\delta^{18}O_{isoGSM,pw}$ vs. T_{obs}	Yining	−0.16	0.34	0.18	0.28	0.25	0.12	0.03	0.84	0.28	0.07
	Bayanbulak	0.14	0.38	0.03	0.83	0.09	0.56	0.05	0.74	0.23	0.14
	Tianchi	−0.22	0.17	0.12	0.47	0.06	0.69	−0.05	0.74	−0.02	0.92
	Yiwu	−0.11	0.51	−0.04	0.79	0.04	0.81	−0.04	0.78	−0.11	0.49
$\delta^{18}O_{obs,p}$ vs. T_{obs}	Urumqi	0.11	0.73	−0.05	0.87	−0.35	0.29	0.29	0.37	−0.06	0.84

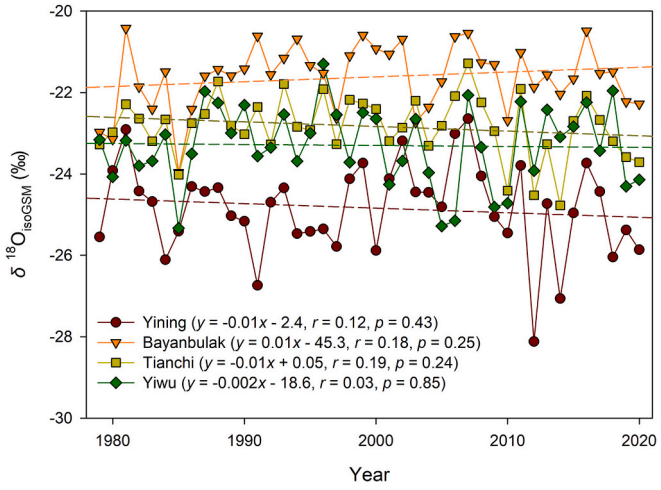

Fig. 5. Interannual variations of isoGSM2-simulated precipitable water $\delta^{18}O$ at typical stations from 1979 to 2020. The annual value is weighted using the observed precipitation amount. The linear trends at each station are also provided as dashed lines.

moisture transport should be examined.

3.3. Linkage between water isotopes and water vapor flux

The Tianshan Mountains are controlled by the mid-latitude Westerlies all year around (Fig. S6). To understand forcing mechanisms behind interannual variation in $\delta^{18}O$ values in atmospheric water, we plotted the correlation between a time series of annual mean $\delta^{18}O$ values at each of four stations and zonal (Fig. 6) or meridional (Fig. 7) water vapor flux for the surrounding region from 1979 to 2020. For the zonal water vapor flux (westerly wind is defined as positive), there is a positive correlation for all four stations along the westerly belt (Fig. 6). Along the mid-latitude westerly wind path around 40°N, the significant correlation generally occurs from the Caspian to the Tianshan Mountains (between 50°E and 80°E), and the nonsignificant positive correlation stretches further to Europe. For meridional water vapor flux (Fig. 7) (southerly wind is defined as positive), there is always a significant positive correlation centralized at around 70°E along the upstream direction (westerly wind) for each station. For the southwestern directions to the Tianshan Mountains, there are also some positive correlations between southerly vapor flux and precipitable water isotope compositions.

In Figs. 6 and 7, the upstream western direction from the Caspian Sea (between 35°N and 50°N, 50°E and 80°E) is a critical area controlling the interannual variability of precipitable water isotopes in the Tianshan Mountains. For this critical region, there is a positive correlation between isotopes and westerly (and southernly) wind. In previous work on

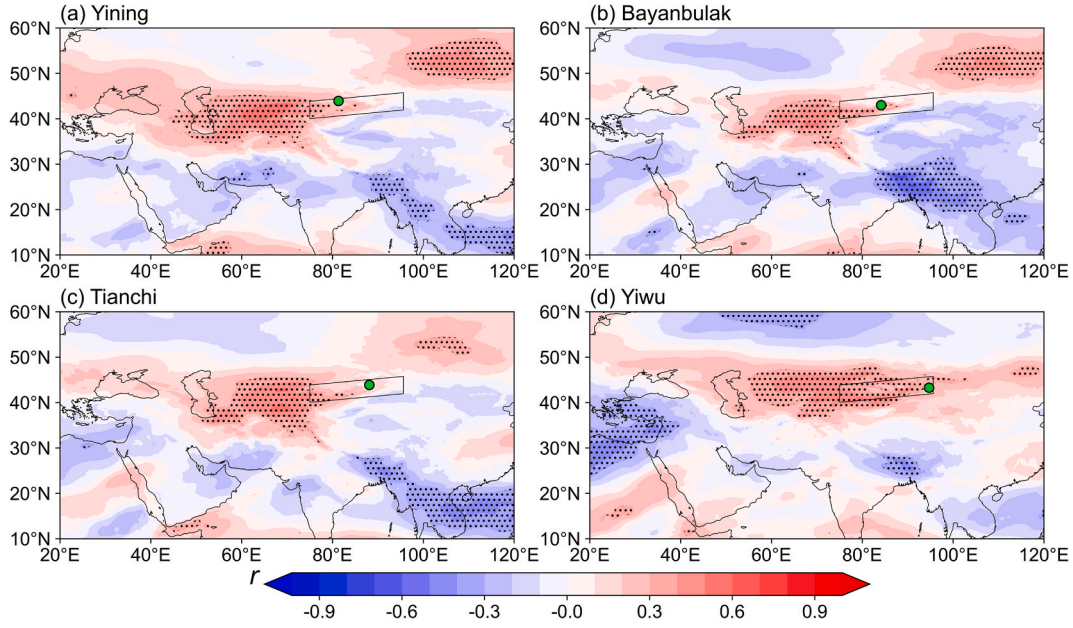

Fig. 6. Spatial distributions of correlation coefficient (*r*) between isoGSM2-simulated weighted $\delta^{18}O$ in precipitable water at each station (a. Yining, b. Bayanbulak, c. Tianchi, and d. Yiwu) and ERA5-derived zonal water vapor flux for the surrounding area on an interannual scale from 1979 to 2020. The black dots denote statistical significance that exceeds the 0.05 level. The positive zonal fluxes indicate wind blowing from west to east.

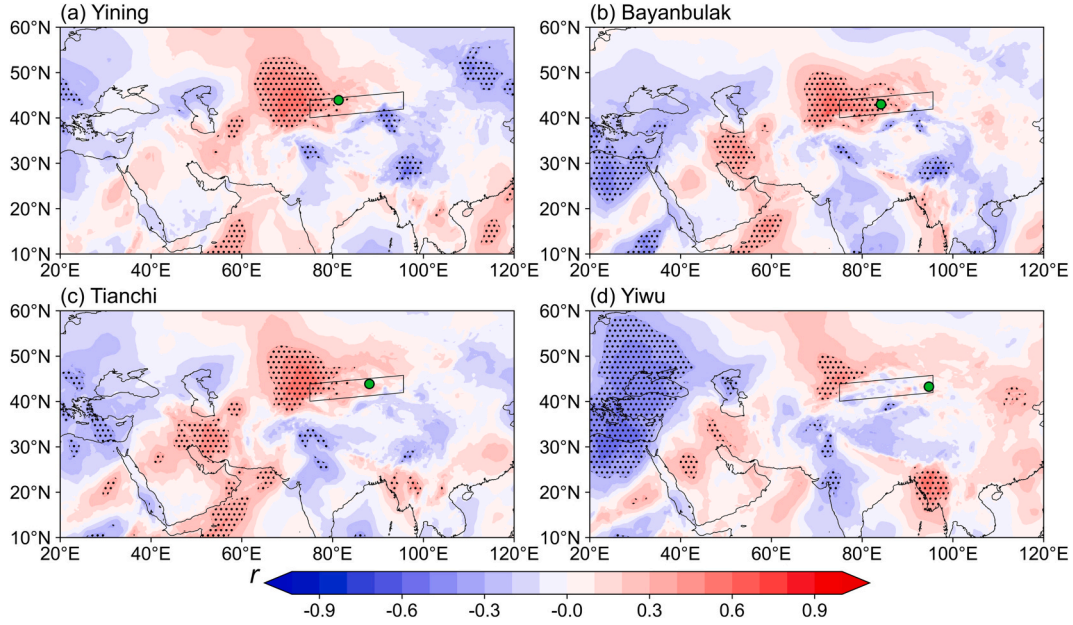

Fig. 7. Spatial distributions of correlation coefficient (r) between isoGSM2-simulated weighted $\delta^{18}O$ in precipitable water at each station (a. Yining, b. Bayanbulak, c. Tianchi, and d. Yiwu) and ERA5-derived meridional water vapor flux for the surrounding area on an interannual scale from 1979 to 2020. The black dots denote statistical significance that exceeds the 0.05 level. The positive meridional fluxes indicate wind blowing from south to north.

specific humidity-adjusted air trajectories (Wang et al., 2017), the backward trajectories of heavy precipitation events in the Tianshan Mountains generally fell in this critical region. Considering the Asian continent as an interaction area of Westerlies Asia and Monsoonal Asia (Chen et al., 2019), this critical area identified here is consistent with the core area of the Westerlies-dominated climate regime. We also noticed that although the four stations selected in the study are approximately 1000 km in distance from west to east, the main moisture regime controlling isotopes in water vapor across the Tianshan Mountains are similar on an annual basis.

3.4. Water vapor flux difference between enriched and depleted years

To identify the interannual differences between moisture regime and isotopic composition, the isoGSM2-based five years with the most enriched (and depleted) annual average precipitable water $\delta^{18}O$ values were selected for each station. Table 2 shows the observed air temperature at typical meteorological stations (Yining, Bayanbulak, Tianchi, Yiwu and Urumqi) during the enriched and depleted years. For the annual series, the Tianchi and Urumqi stations in enriched years are much colder than those in depleted years, and the temperature differences are −0.48 °C and − 0.46 °C, respectively, which is the opposite of the temperature effect. In Yining, the enriched years correspond to a slightly warmer year, which is only 0.14 °C (close to the resolution of 0.1 °C in temperature observations) warmer than the depleted years. For the summer series, most stations still have a lower temperature during the enriched years. The temperature effect cannot be found in the observed air temperature records during the enriched and depleted years. Figs. S7 and S8 show the spatial patterns of annual and summer mean temperature differences derived from ERA climate reanalysis. However, the is no spatially coherent positive difference (enriched years minus depleted years) in temperature across the Tianshan Mountains.

Table 2
Annual and summer mean air temperature observed during the enriched and depleted years and the difference (enriched years minus depleted years) of typical stations.

Period	Year	Temperature (°C)				
		Yining	Bayanbulak	Tianchi	Yiwu	Urumqi
Annual	Enriched years	9.68	−4.43	2.21	4.30	1.50
	Depleted years	9.54	−4.42	2.69	4.32	1.95
	Difference	0.14	−0.01	−0.48	−0.02	−0.46
Summer	Enriched years	22.34	10.43	14.24	17.54	12.07
	Depleted years	22.57	10.31	14.72	18.49	12.58
	Difference	−0.24	0.13	−0.47	−0.95	−0.51

Here we applied clustered backward trajectories to examine the difference in spatial positions during enriched and depleted years. As shown in Fig. S9, three main branches are identified for both enriched and depleted conditions. Two trajectories with relatively long distances are generally consistent with the southwestern and northwestern directions from lower (brown and yellow, in enriched and depleted years) and higher (dark and light green) latitudes, respectively, and the other trajectory is from the relatively nearby regions (purple and pink). For the southwestern trajectory clusters, the enriched years usually correspond to lower mean latitudes along the paths than the depleted years. This pattern is clear at both 500 m and 1500 m above ground level. The southward movement of air mass in the critical area corresponds to enriched isotopes on an annual basis. However, the southward distance shown in Fig. S9 is not very large from depleted to enriched years, indicating the dominant role of mid-latitude westerly.

The reanalysis-based water vapor flux reflects the integrated result of moisture loading and air movement. By direct comparison, it is difficult to observe the difference between the isotopically enriched (Fig. S10) and depleted (Fig. S11) years at each station, as their patterns are similar to the main transport of water vapor via the Westerlies. When calculating the spatial difference in water vapor flux between the enriched and depleted years to the target station (Fig. 8), we observed the westerly (or southwesterly) winds at the upstream critical area from the Caspian Sea to the Tianshan Mountains. As shown in Fig. 8, the westerly wind-derived moisture transport at the critical area is enhanced when $\delta^{18}O$ values are high. When we examine the zonal (Fig. S12) and meridional (Fig. S13) moisture flux, we can also see the difference in enhanced westerly and southerly moisture at the critical region.

Generally, water vapor $\delta^{18}O$ after long-distance transport is more

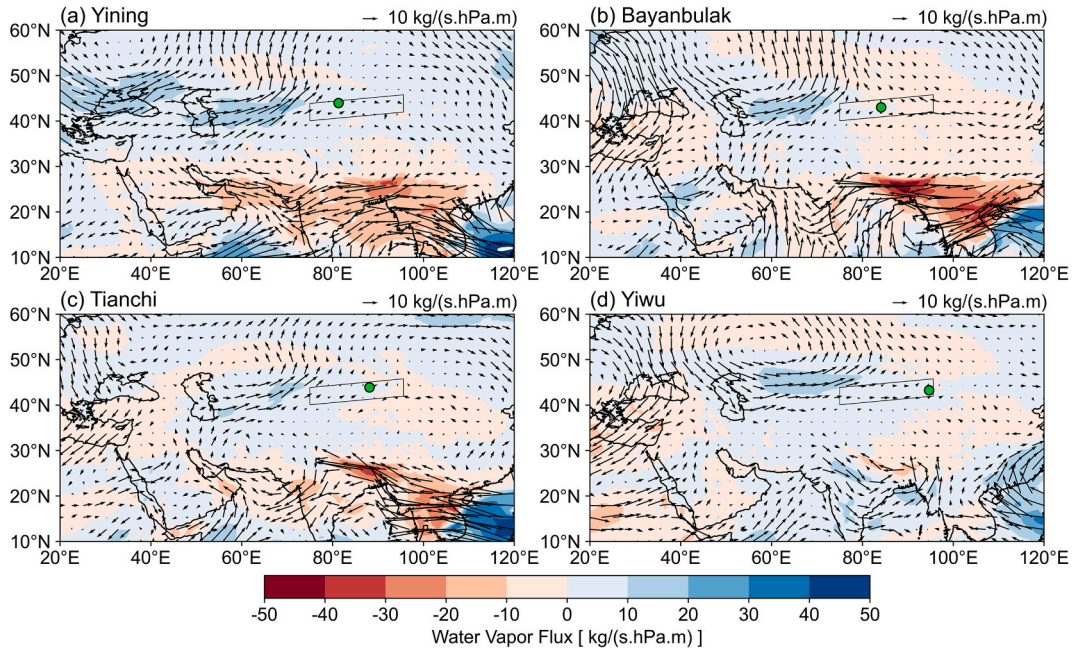

Fig. 8. IsoGSM2-simulated annual-mean water vapor flux difference (both shades and vectors) between enriched and depleted years at each station (a. Yining, b. Bayanbulak, c. Tianchi, and d. Yiwu). The water vapor flux in five enriched years minus the water vapor flux in five depleted years.

negative than water vapor $\delta^{18}O$ near the ocean due to the continental effect, which is characterized by more Rayleigh distillation of the vapor (Rozanski et al., 1993). In this study, the trajectory of westerly moisture traveling to the Tianshan Mountains changes interannually. Along the westerly path at lower latitudes with strong evaporation, the water vapor is usually enriched in heavy isotopes, which is evident from the isoscape of precipitation (Bowen and Wilkinson, 2002). For the critical region, during enriched years, the mid-latitude westerly wind and moisture flux are stronger (Fig. S10), and the southerly wind and moisture flux is also enhanced (Fig. S11), leading to more vapor from the lower latitudes that can be transported to the Tianshan Mountains via the westerly belt. In contrast, during the depleted years, when the moisture transport of the westerly is weakened along the upstream direction (Fig. S10), the water vapor path is slightly northerly (Fig. S11), and less vapor evaporated from lower latitudes can be incorporated into the westerly moisture.

Previous studies (Liu et al., 2015; Shi et al., 2021) mentioned the relationship between the westerly belt and isotopes in atmospheric water in Central Asia, while a comprehensive understanding of the interaction between Westerlies and monsoon is still needed using modern precipitation isotopes. The difference in water vapor flux between high and low $\delta^{18}O$ years reflects the strength of both Westerlies and monsoon circulations (Fig. 8). When the Westerlies intensified, the Indian summer monsoon is usually weak, and the mid-latitude Westerlies carry more water vapor from the lower latitude, resulting in more positive $\delta^{18}O$ values of precipitation. Contrarily, low $\delta^{18}O$ years are associated with weak Westerlies. Our results suggest that, on interannual timescales, the atmospheric circulation, instead of the temperature effect, is responsible for variation in $\delta^{18}O$ in Central Asia. Our result is supported by recent paleoclimate studies based on speleothem and other geological records, which showed similar results that the interaction of the Westerlies and monsoonal moisture impacts the paleo-precipitation $\delta^{18}O$ values in arid Central Asia (Chen et al., 2019, 2022b; Liu et al., 2020). For example, Zhang et al. (2017) showed that the intensified moisture with enriched isotopes transport from lower latitudes was the key source of the increased Central Asian precipitation from the early Holocene to the late Holocene. These suggest that the supra-regional circulation-caused moisture source and trajectory variations are responsible for changes in $\delta^{18}O$ on various timescales. Consequently, we conclude that observed interannual changes in $\delta^{18}O$ in Central Asia are caused by the path of Westerlies (the jet stream) and the amount of water vapor flux, which provides modern climate evidence for the Holocene moisture variations revealed by paleoclimate proxies in arid Central Asia.

4. Conclusions

To understand the environmental controls of stable isotopes in atmospheric water in Central Asia with limited in-situ observations, an isotope-enabled climate model was used to revisit the temperature effect on the intra- and interannual scales. The main factor controlling the variation of $\delta^{18}O$ on the intra-annual scale is seasonal temperature changes (also known as the temperature effect). In arid Central Asia, which is dominated by Westerlies, interannual variation in $\delta^{18}O$ does not significantly correlate with temperature, as it does on intra-annual scales. This is also supported by the observations at a typical station. Instead, there is a strong correlation between westerly (and southerly) water vapor flux and $\delta^{18}O$ on the interannual scale especially for the critical area from the Caspian Sea to the Tianshan Mountains (between 35°N–50°N and 50°E–80°E). We interpret variation in $\delta^{18}O$ on interannual time scales to be the result of a westerly vapor flux and the potential supplement of enriched water vapor. When the Westerlies are enhanced, the Westerlies belt carries more water vapor with enriched isotope via a slightly southward trajectory, leading to more enriched $\delta^{18}O$ values of atmospheric water in Central Asia. Contrarily, when the Westerlies belt moves north, it carries more long-distance transported water vapor from the higher latitudes, resulting in lower $\delta^{18}O$ values. The modelling shows that interannual variation of isotopes in atmospheric water in arid Central Asia may be not only controlled by temperature, and reflects the changes in mid-latitude Westerlies circulation, which should be taken into account when interpreting stable isotope climate proxies in Central Asia. More long-term observations are still needed to distinguish the possible contribution of the temperature effect and circulation effect.

CRediT authorship contribution statement

Shengjie Wang: Conceptualization, Data curation, Formal analysis,

Funding acquisition, Investigation, Methodology, Validation, Visualization, Writing – original draft, Writing – review & editing. **Gahong Yang:** Conceptualization, Data curation, Investigation, Methodology, Validation, Visualization, Writing – original draft, Writing – review & editing. **John Bershaw:** Methodology, Validation, Writing – review & editing, Investigation. **Xiaokang Liu:** Methodology, Validation, Writing – review & editing, Investigation. **Kei Yoshimura:** Methodology, Validation, Writing – review & editing. **Yanqiong Xiao:** Investigation, Writing – original draft. **Mingjun Zhang:** Conceptualization, Investigation, Methodology, Writing – original draft, Writing – review & editing.

Declaration of competing interest

The authors declare that they have no known competing financial interests or personal relationships that could have appeared to influence the work reported in this paper.

Data availability

The stable isotope simulation of isoGSM2 is online available at http://isotope.iis.u-tokyo.ac.jp/~kei/tmp/isogsm2. The ERA5 reanalysis is provided by the European Centre for Medium-Range Weather Forecasts (https://cds.climate.copernicus.eu/cdsapp#!/dataset/reanalysis-era5-pressure-levels-monthly-means). Observed meteorological data is available at the Resources and Environment Science and Data Center (https://www.resdc.cn/data.aspx?DATAID=230). The Global Unified Gauge-based Analysis of Daily Precipitation is available at NOAA (https://downloads.psl.noaa.gov/Datasets/cpc_global_precip). The HYSPLIT model is available at https://www.ready.noaa.gov/HYSPLIT_hytrial.php, and the HYSPLIT-compatible NCEP/NCAR global reanalysis data is available at https://www.ready.noaa.gov/archives.php.

Acknowledgments

This work is supported by the National Natural Science Foundation of China (No. 42261008 and 41971034), the Foundation for Distinguished Young Scholars of Gansu Province (20JR10RA112) and the Gansu Provincial Natural Science Foundation (22JR5RA074). Thanks for the useful suggestions from Camille Risi (Laboratoire de Météorologie Dynamique) and Shaohua Dang (Tongji University).

Appendix A. Supplementary data

Supplementary data to this article can be found online at https://doi.org/10.1016/j.gloplacha.2024.104367.

References

Araguás-Araguás, L., Froehlich, K., Rozanski, K., 1998. Stable isotope composition of precipitation over Southeast Asia. J. Geophys. Res. Atmos. 103, 28721–28742. https://doi.org/10.1029/98JD02582.

Baker, A., Hartmann, A., Duan, W., Hankin, S., Comas-Bru, L., Cuthbert, M.O., Treble, P. C., Banner, J., Genty, D., Baldini, L.M., Bartolomé, M., Moreno, A., Pérez-Mejías, C., Werner, M., 2019. Global analysis reveals climatic controls on the oxygen isotope composition of cave drip water. Nat. Commun. 10, 2984. https://doi.org/10.1038/s41467-019-11027-w.

Bershaw, J., 2018. Controls on deuterium excess across Asia. Geosciences 8, 257. https://doi.org/10.3390/geosciences8070257.

Bowen, G.J., Wilkinson, B., 2002. Spatial distribution of $\delta^{18}O$ in meteoric precipitation. Geology 30, 315–318. https://doi.org/10.1130/0091-7613(2002)030<0315:SDOOIM>2.0.CO;2.

Bowen, G.J., Cai, Z., Fiorella, R.P., Putman, A.L., 2019. Isotopes in the water cycle: regional- to global-scale patterns and applications. Annu. Rev. Earth Planet. Sci. 47, 453–479. https://doi.org/10.1146/annurev-earth-053018-060220.

Bühler, J.C., Axelsson, J., Lechleitner, F.A., Fohlmeister, J., LeGrande, A.N., Midhun, M., Sjolte, J., Werner, M., Yoshimura, K., Rehfeld, K., 2022. Investigating stable oxygen and carbon isotopic variability in speleothem records over the last millennium using multiple isotope-enabled climate models. Clim. Past 18, 1625–1654. https://doi.org/10.5194/cp-18-1625-2022.

Cai, Y., Chiang, J.C.H., Breitenbach, S.F.M., Tan, L., Cheng, H., Edwards, R.L., An, Z., 2017. Holocene moisture changes in western China, Central Asia, inferred from stalagmites. Quat. Sci. Rev. 158, 15–28. https://doi.org/10.1016/j.quascirev.2016.12.014.

Chen, M., Shi, W., Xie, P., Silva, V.B., Kousky, V.E., Wayne Higgins, R., Janowiak, J.E., 2008. Assessing objective techniques for gauge-based analyses of global daily precipitation. J. Geophys. Res. 113, D04110. https://doi.org/10.1029/2007JD009132.

Chen, F., Chen, J., Huang, W., Chen, S., Huang, X., Jin, L., Jia, J., Zhang, X., An, C., Zhang, J., 2019. Westerlies Asia and monsoonal Asia: spatiotemporal differences in climate change and possible mechanisms on decadal to sub-orbital timescales. Earth Sci. Rev. 192, 337–354. https://doi.org/10.1016/j.earscirev.2019.03.005.

Chen, F., Chen, J., Huang, W., 2021. Weakened East Asian summer monsoon triggers increased precipitation in Northwest China. Sci. China Earth Sci. 64, 835–837. https://doi.org/10.1007/s11430-020-9731-7.

Chen, F., Yuan, Y., Trouet, V., Büntgen, U., Esper, J., Chen, F., Yu, S., Shen, M., Zhang, R., Shang, H., Chen, Y., Zhang, H., 2022a. Ecological and societal effects of Central Asian streamflow variation over the past eight centuries. Npj Clim. Atmos. Sci. 5, 27. https://doi.org/10.1038/s41612-022-00239-5.

Chen, S., Chen, J., Lv, F., Liu, X., Huang, W., Wang, T., Liu, J., Hou, J., Chen, F., 2022b. Holocene moisture variations in arid Central Asia: reassessment and reconciliation. Quat. Sci. Rev. 297, 107821 https://doi.org/10.1016/j.quascirev.2022.107821.

Chen, Y., Fang, G., Hao, H., Wang, X., 2022c. Water use efficiency data from 2000 to 2019 in measuring progress towards SDGs in Central Asia. Big Earth Data 6, 90–102. https://doi.org/10.1080/20964471.2020.1851891.

Cheng, H., Edwards, R.L., Sinha, A., Spotl, C., Yi, L., Chen, S., Kelly, M., Kathayat, G., Wang, X., Li, X., Kong, X., Wang, Y., Ning, Y., Zhang, H., 2016a. The Asian monsoon over the past 640,000 years and ice age terminations. Nature 534, 640–646. https://doi.org/10.1038/nature18591.

Cheng, H., Spoetl, C., Breitenbach, S.F.M., Sinha, A., Wassenburg, J.A., Jochum, K.P., Scholz, D., Li, X.L., Yi, L., Peng, Y.B., Lv, Y.B., Zhang, P.Z., Votintseva, A., Loginov, V., Ning, Y.F., Kathayat, G., Edwards, R.L., 2016b. Climate variations of Central Asia on orbital to millennial timescales. Sci. Rep. 6, 36975. https://doi.org/10.1038/srep36975.

Chiang, J.C.H., Herman, M.J., Yoshimura, K., Fung, I.Y., 2020. Enriched East Asian oxygen isotope of precipitation indicates reduced summer seasonality in regional climate and westerlies. Proc. Natl. Acad. Sci. 117, 14745–14750. https://doi.org/10.1073/pnas.1922602117.

Crawford, J., Hollins, S.E., Meredith, K.T., Hughes, C.E., 2017. Precipitation stable isotope variability and subcloud evaporation processes in a semi-arid region. Hydrol. Process. 31, 20–34. https://doi.org/10.1002/hyp.10885.

Dar, S.S., Ghosh, P., Hillaire-Marcel, C., 2021. Convection, terrestrial recycling and oceanic moisture regulate the isotopic composition of precipitation at Srinagar, Kashmir. J. Geophys. Res. Atmos. 126 https://doi.org/10.1029/2020JD032853 e2020JD032853.

Gao, J., Risi, C., Masson-Delmotte, V., He, Y., Xu, B., 2016. Southern Tibetan Plateau ice core $\delta^{18}O$ reflects abrupt shifts in atmospheric circulation in the late 1970s. Clim. Dyn. 46, 291–302. https://doi.org/10.1007/s00382-015-2584-3.

Gimeno, L., Vazquez, M., Eiras-Barca, J., Sori, R., Stojanovic, M., Algarra, I., Nieto, R., Ramos, A.M., Duran-Quesada, A.M., Dominguez, F., 2020. Recent progress on the sources of continental precipitation as revealed by moisture transport analysis. Earth Sci. Rev. 201, 103070 https://doi.org/10.1016/j.earscirev.2019.103070.

Graf, P., Wernli, H., Pfahl, S., Sodemann, H., 2019. A new interpretative framework for below-cloud effects on stable water isotopes in vapour and rain. Atmos. Chem. Phys. 19, 747–765. https://doi.org/10.5194/acp-19-747-2019.

Guan, X., Yao, J., Schneider, C., 2022. Variability of the precipitation over the Tianshan Mountains, Central Asia. Part II: multi-decadal precipitation trends and their association with atmospheric circulation in both the winter and summer seasons. Int. J. Climatol. 42, 139–156. https://doi.org/10.1002/joc.7236.

Gui, J., Li, Z., Feng, Q., Zhang, B., Xue, J., Gao, W., Li, Y., Liang, P., Nan, F., 2022. Water resources significance of moisture recycling in the transition zone between Tibetan Plateau and arid region by stable isotope tracing. J. Hydrol. 605, 127350 https://doi.org/10.1016/j.jhydrol.2021.127350.

Hersbach, H., Bell, B., Berrisford, P., Hirahara, S., Horányi, A., Muñoz-Sabater, J., Nicolas, J., Peubey, C., Radu, R., Schepers, D., Simmons, A., Soci, C., Abdalla, S., Abellan, X., Balsamo, G., Bechtold, P., Biavati, G., Bidlot, J., Bonavita, M., De Chiara, G., Dahlgren, P., Dee, D., Diamantakis, M., Dragani, R., Flemming, J., Forbes, R., Fuentes, M., Geer, A., Haimberger, L., Healy, S., Hogan, R.J., Hólm, E., Janisková, M., Keeley, S., Laloyaux, P., Lopez, P., Lupu, C., Radnoti, G., de Rosnay, P., Rozum, I., Vamborg, F., Villaume, S., Thépaut, J.N., 2020. The ERA5 global reanalysis. Q. J. R. Meteorol. Soc. 146, 1999–2049. https://doi.org/10.1002/qj.3803.

Huang, Y., Xiao, C.D., Su, B., 2022. Importance and vulnerability of water towers across Northwest China. Adv. Clim. Chang. Res. 13, 63–72. https://doi.org/10.1016/j.accre.2021.12.002.

IAEA, 2022. Water Isotope System for Data Analysis, Visualization and Electronic Retrieval. accessed 25 August 2022,. https://nucleus.iaea.org/wiser/index.aspx.

Kalnay, E., Kanamitsu, M., Kistler, R., Collins, W., Deaven, D., Gandin, L., Iredell, M., Saha, S., White, G., Woollen, J., Zhu, Y., Chelliah, M., Ebisuzaki, W., Higgins, W., Janowiak, J., Mo, K.C., Ropelewski, C., Wang, J., Leetmaa, A., Reynolds, R., Jenne, R., Joseph, D., 1996. The NCEP/NCAR 40-year reanalysis project. Bull. Am. Meteorol. Soc. 77, 437–472. https://doi.org/10.1175/1520-0477(1996)077<0437:TNYRP>2.0.CO;2.

Kathayat, G., Sinha, A., Breitenbach, S.F., Tan, L., Spötl, C., Li, H., Dong, X., Zhang, H., Ning, Y., Allan, R.J., 2022. Protracted Indian monsoon droughts of the past

millennium and their societal impacts. Proc. Natl. Acad. Sci. 119, e2207487119 https://doi.org/10.1073/pnas.2207487119.
Konapala, G., Mishra, A.K., Wada, Y., Mann, M.E., 2020. Climate change will affect global water availability through compounding changes in seasonal precipitation and evaporation. Nat. Commun. 11, 3044. https://doi.org/10.1038/s41467-020-16757-w.
Kong, Y., Pang, Z., Froehlich, K., 2013. Quantifying recycled moisture fraction in precipitation of an arid region using deuterium excess. Tellus Ser. B Chem. Phys. Meteorol. 65, 19251. https://doi.org/10.3402/tellusb.v65i0.19251.
Liu, J., Song, X., Yuan, G., Sun, X., Yang, L., 2014. Stable isotopic compositions of precipitation in China. Tellus Ser. B Chem. Phys. Meteorol. 66, 22567. https://doi.org/10.3402/tellusb.v66.22567.
Liu, X., Rao, Z., Zhang, X., Huang, W., Chen, J., Chen, F., 2015. Variations in the oxygen isotopic composition of precipitation in the Tianshan Mountains region and their significance for the Westerly circulation. J. Geogr. Sci. 25, 801–816. https://doi.org/10.1007/s11442-015-1203-x.
Liu, X., Liu, J., Shen, C.C., Yang, Y., Chen, J., Chen, S., Wang, X., Wu, C.C., Chen, F., 2020. Inconsistency between records of $\delta^{18}O$ and trace element ratios from stalagmites: evidence for increasing mid-late Holocene moisture in arid Central Asia. Holocene 30, 369–379. https://doi.org/10.1177/0959683619887431.
Liu, Z., Zhang, X., Xiao, Z., He, X., Rao, Z., Guan, H., 2023. The relations between summer droughts/floods and oxygen isotope composition of precipitation in the Dongting Lake basin. Int. J. Climatol. 43, 3590–3604. https://doi.org/10.1002/joc.8047.
Man, W., Zhou, T., Jiang, J., Zuo, M., Hu, J., 2022. Moisture sources and climatic controls of precipitation stable isotopes over the Tibetan Plateau in water-tagging simulations. J. Geophys. Res. Atmos. 127 https://doi.org/10.1029/2021JD036321 e2021JD036321.
Markle, B.R., Steig, E.J., 2022. Improving temperature reconstructions from ice-core water-isotope records. Clim. Past 18, 1321–1368. https://doi.org/10.5194/cp-18-1321-2022.
Pang, Z., Kong, Y., Froehlich, K., Huang, T., Yuan, L., Li, Z., Wang, F., 2011. Processes affecting isotopes in precipitation of an arid region. Tellus Ser. B Chem. Phys. Meteorol. 63, 352–359. https://doi.org/10.1111/j.1600-0889.2011.00532.x.
Parker, S.E., Harrison, S.P., Comas-Bru, L., Kaushal, N., LeGrande, A.N., Werner, M., 2021. A data–model approach to interpreting speleothem oxygen isotope records from monsoon regions. Clim. Past 17, 1119–1138. https://doi.org/10.5194/cp-17-1119-2021.
Peng, D., Zhou, T., Zhang, L., 2020. Moisture sources associated with precipitation during dry and wet seasons over Central Asia. J. Clim. 33, 10755–10771. https://doi.org/10.1175/JCLI-D-20-0029.1.
Putman, A.L., Fiorella, R.P., Bowen, G.J., Cai, Z., 2019. A global perspective on local meteoric water lines: meta-analytic insight into fundamental controls and practical constraints. Water Resour. Res. 55, 6896–6910. https://doi.org/10.1029/2019WR025181.
Rao, Z., Wu, D., Shi, F., Guo, H., Cao, J., Chen, F., 2019. Reconciling the 'westerlies' and 'monsoon' models: a new hypothesis for the Holocene moisture evolution of the Xinjiang region, NW China. Earth Sci. Rev. 191, 263–272. https://doi.org/10.1016/j.earscirev.2019.03.002.
Risi, C., Noone, D., Frankenberg, C., Worden, J., 2013. Role of continental recycling in intraseasonal variations of continental moisture as deduced from model simulations and water vapor isotopic measurements. Water Resour. Res. 49, 4136–4156. https://doi.org/10.1002/wrcr.20312.
Rozanski, K., Araguás-Araguás, L., Gonfiantini, R., 1993. Isotopic patterns in modern global precipitation. In: Swart, P.K., Lohmann, K.C., Mckenzie, J., Savin, S. (Eds.), Climate Change in Continental Isotopic Records. American Geophysical Union, pp. 1–36. https://doi.org/10.1029/GM078p0001.
Salati, E., Dall'Olio, A., Matsui, E., Gat, J.R., 1979. Recycling of water in the Amazon basin: an isotopic study. Water Resour. Res. 15, 1250–1258. https://doi.org/10.1029/WR015i005p01250.
Shen, Z., Zhang, Q., Singh, V.P., Pokhrel, Y., Li, J., Xu, C.Y., Wu, W., 2022. Drying in the low-latitude Atlantic Ocean contributed to terrestrial water storage depletion across Eurasia. Nat. Commun. 13, 1849. https://doi.org/10.1038/s41467-022-29544-6.
Shi, Y., Wang, S., Wang, L., Zhang, M., Argiriou, A.A., Song, Y., Lei, S., 2021. Isotopic evidence in modern precipitation for the westerly meridional movement in Central Asia. Atmos. Res. 259, 105698 https://doi.org/10.1016/j.atmosres.2021.105698.
Shi, M., Worden, J.R., Bailey, A., Noone, D., Risi, C., Fu, R., Worden, S., Herman, R., Payne, V., Pagano, T., Bowman, K., Bloom, A.A., Saatchi, S., Liu, J., Fisher, J.B., 2022. Amazonian terrestrial water balance inferred from satellite-observed water vapor isotopes. Nat. Commun. 13, 2686. https://doi.org/10.1038/s41467-022-30317-4.
Song, Y., Wang, S., Zhang, M., Shi, Y., 2022. Stable isotopes of precipitation in the eastern Tarim River basin and water vapor sources. Environ. Sci. 43, 199–209. https://doi.org/10.13227/j.hjkx.202104210.
Stein, A.F., Draxler, R.R., Rolph, G.D., Stunder, B.J.B., Cohen, M.D., Ngan, F., 2015. NOAA's HYSPLIT atmospheric transport and dispersion modeling system. Bull. Am. Meteorol. Soc. 96, 2059–2077. https://doi.org/10.1175/BAMS-D-14-00110.1.
Sun, C., Chen, Y., Li, W., Li, X., Yang, Y., 2016. Isotopic time series partitioning of streamflow components under regional climate change in the Urumqi River, Northwest China. Hydrol. Sci. J. 61, 1443–1459. https://doi.org/10.1080/02626667.2015.1031757.
Sun, C., Chen, Y., Li, J., Chen, W., Li, X., 2019. Stable isotope variations in precipitation in the northwesternmost Tibetan Plateau related to various meteorological controlling factors. Atmos. Res. 227, 66–78. https://doi.org/10.1016/j.atmosres.2019.04.026.
Thackeray, C.W., Hall, A., Norris, J., Chen, D., 2022. Constraining the increased frequency of global precipitation extremes under warming. Nat. Clim. Chang. 12, 441–448. https://doi.org/10.1038/s41558-022-01329-1.
Thompson, L.G., Yao, T., Davis, M.E., Henderson, K.A., Mosley-Thompson, E., Lin, P.N., Beer, J., Synal, H.A., Cole-Dai, J., Bolzan, J.F., 1997. Tropical climate instability: the last glacial cycle from a Qinghai-Tibetan ice core. Science 276, 1821–1825. https://doi.org/10.1126/science.276.5320.1821.
Thompson, L.G., Yao, T., Davis, M.E., Mosley-Thompson, E., Wu, G., Porter, S.E., Xu, B., Lin, P.N., Wang, N., Beaudon, E., 2018. Ice core records of climate variability on the Third Pole with emphasis on the Guliya ice cap, western Kunlun Mountains. Quat. Sci. Rev. 188, 1–14. https://doi.org/10.1016/j.quascirev.2018.03.003.
Tian, L., Yao, T., Li, Z., MacClune, K., Wu, G., Xu, B., Li, Y., Lu, A., Shen, Y., 2006. Recent rapid warming trend revealed from the isotopic record in Muztagata ice core, eastern Pamirs. J. Geophys. Res. 111, D13103. https://doi.org/10.1029/2005JD006249.
Tian, L., Yao, T., MacClune, K., White, J., Schilla, A., Vaughn, B., Vachon, R., Ichiyanagi, K., 2007. Stable isotopic variations in West China: a consideration of moisture sources. J. Geophys. Res. Atmos. 112, D10112. https://doi.org/10.1029/2006JD007718.
Wang, S., Zhang, M., Hughes, C.E., Zhu, X., Dong, L., Ren, Z., Chen, F., 2016. Factors controlling stable isotope composition of precipitation in arid conditions: an observation network in the Tianshan Mountains, Central Asia. Tellus Ser. B Chem. Phys. Meteorol. 68, 26206. https://doi.org/10.3402/tellusb.v68.26206.
Wang, S., Zhang, M., Crawford, J., Hughes, C.E., Du, M., Liu, X., 2017. The effect of moisture source and synoptic conditions on precipitation isotopes in arid Central Asia. J. Geophys. Res. Atmos. 122, 2667–2682. https://doi.org/10.1002/2015JD024626.
Wang, L., Dong, Y., Han, D., Xu, Z., 2019. Stable isotopic compositions in precipitation over wet island in Central Asia. J. Hydrol. 573, 581–591. https://doi.org/10.1016/j.jhydrol.2019.04.005.
Wang, S., Jiao, R., Zhang, M., Crawford, J., Hughes, C.E., Chen, F., 2021. Changes in below-cloud evaporation affect precipitation isotopes during five decades of warming across China. J. Geophys. Res. Atmos. 126 https://doi.org/10.1029/2020JD033075 e2020JD033075.
Wang, S., Wang, L., Zhang, M., Shi, Y., Hughes, C.E., Crawford, J., Zhou, J., Qu, D., 2022. Quantifying moisture recycling of a leeward oasis in arid Central Asia using a Bayesian isotopic mixing model. J. Hydrol. 613, 128459 https://doi.org/10.1016/j.jhydrol.2022.128459.
Welp, L.R., Olson, E.J., Valdivia, A.L., Larico, J.R., Arhuire, E.P., Paredes, L.M., DeGraw, J.T., Michalski, G.M., 2022. Reinterpreting precipitation stable water isotope variability in the Andean Western Cordillera due to sub-seasonal moisture source changes and sub-cloud evaporation. Geophys. Res. Lett. 49 https://doi.org/10.1029/2022GL099876 e2022GL099876.
Wu, P., Ding, Y., Liu, Y., Li, X., 2019. The characteristics of moisture recycling and its impact on regional precipitation against the background of climate warming over Northwest China. Int. J. Climatol. 39, 5241–5255. https://doi.org/10.1002/joc.6136.
Xu, G., Liu, X., Qin, D., Chen, T., Wang, W., Wu, G., Sun, W., An, W., Zeng, X., 2014. Tree-ring $\delta^{18}O$ evidence for the drought history of eastern Tianshan Mountains, Northwest China since 1700 AD. Int. J. Climatol. 34, 3336–3347. https://doi.org/10.1002/joc.3911.
Xu, C., Sano, M., Dimri, A.P., Ramesh, R., Nakatsuka, T., Shi, F., Guo, Z., 2018. Decreasing Indian summer monsoon on the northern Indian sub-continent during the last 180 years: evidence from five tree-ring cellulose oxygen isotope chronologies. Clim. Past 14, 653–664. https://doi.org/10.5194/cp-14-653-2018.
Xu, C., Zhao, Q., An, W., Wang, S., Tan, N., Sano, M., Nakatsuka, T., Borhara, K., Guo, Z., 2021. Tree-ring oxygen isotope across monsoon Asia: common signal and local influence. Quat. Sci. Rev. 269, 107156 https://doi.org/10.1016/j.quascirev.2021.107156.
Xue, D., Gui, D., Dai, H., Liu, Y., Liu, Y., Zhang, L., Ahmed, Z., 2022. Oasis sustainability assessment in arid areas using GRACE satellite data. Environ. Monit. Assess. 194, 361. https://doi.org/10.1007/s10661-022-09929-2.
Yang, S., Zhang, M., Wang, S., 2018. Affecting mechanism of moisture sources of isotopes in precipitation in the Tianshan Mountains based on GCMs and ice core. Arid Zone Res. 35, 425–435. https://doi.org/10.13866/j.azr.2018.02.22.
Yao, T., Masson-Delmotte, V., Gao, J., Yu, W., Yang, X., Risi, C., Sturm, C., Werner, M., Zhao, H., He, Y., Ren, W., Tian, L., Shi, C., Hou, S., 2013. A review of climatic controls on $\delta^{18}O$ in precipitation over the Tibetan Plateau: observations and simulations. Rev. Geophys. 51, 525–548. https://doi.org/10.1002/rog.20023.
Yao, J., Chen, Y., Zhao, Y., Guan, X., Mao, W., Yang, L., 2020. Climatic and associated atmospheric water cycle changes over the Xinjiang, China. J. Hydrol. 585, 124823 https://doi.org/10.1016/j.jhydrol.2020.124823.
Yao, J., Chen, Y., Guan, X., Zhao, Y., Chen, J., Mao, W., 2022. Recent climate and hydrological changes in a mountain–basin system in Xinjiang, China. Earth Sci. Rev. 226, 103957 https://doi.org/10.1016/j.earscirev.2022.103957.
Yoshimura, K., Kanamitsu, M., Noone, D., Oki, T., 2008. Historical isotope simulation using reanalysis atmospheric data. J. Geophys. Res. Atmos. 113, D19108. https://doi.org/10.1029/2008JD010074.
Yu, W., Yao, T., Thompson, L.G., Jouzel, J., Zhao, H., Xu, B., Jing, Z., Wang, N., Wu, G., Ma, Y., 2021. Temperature signals of ice core and speleothem isotopic records from Asian monsoon region as indicated by precipitation $\delta^{18}O$. Earth Planet. Sci. Lett. 554, 116665 https://doi.org/10.1016/j.epsl.2020.116665.
Zhang, X., 2021. Penetration of monsoonal water vapour into arid Central Asia during the Holocene: an isotopic perspective. Quat. Sci. Rev. 251, 106713 https://doi.org/10.1016/j.quascirev.2020.106713.
Zhang, X., Jin, L., Chen, J., Chen, F., Park, W., Schneider, B., Latif, M., 2017. Detecting the relationship between moisture changes in arid Central Asia and East Asia during

the Holocene by model-proxy comparison. Quat. Sci. Rev. 176, 36–50. https://doi.org/10.1016/j.quascirev.2017.09.012.

Zhang, F., Huang, T., Man, W., Hu, H., Long, Y., Li, Z., Pang, Z., 2021. Contribution of recycled moisture to precipitation: a modified D-excess-based model. Geophys. Res. Lett. 48 https://doi.org/10.1029/2021GL095909 e2021GL095909.

Zhang, J., Yu, W., Lewis, S., Thompson, L.G., Bowen, G.J., Yoshimura, K., Cauquoin, A., Werner, M., Chakraborty, S., Jing, Z., Ma, Y., Guo, X., Xu, B., Wu, G., Guo, R., Qu, D., 2023. Controls on stable water isotopes in monsoonal precipitation across the Bay of Bengal: atmosphere and surface analysis. Geophys. Res. Lett. 50 https://doi.org/10.1029/2022GL102229 e2022GL102229.